

Calibration of the ATLAS Hadronic End-Cap Calorimeter

Brettel H., Cwienk W.D., Kurchaninov L., Oberlack H., Schacht P.

Max-Planck-Institute for Physics, Munich, Germany

Jusko A., Strizenec P.

IEP SAS, Kosice, Slovakia

On behalf of the ATLAS HEC Collaboration

Abstract

The calibration chain of the HEC is described. A model based on detailed studies of all individual parts is presented. The characteristics of the steering and data taking system for both the test-beam runs and for the acceptance tests of the HEC modules is summarized. The calibration and signal reconstruction procedure is developed and results of the test-beam data are presented.

1 INTRODUCTION

The calibration of the electronics chain should

- equalize the gains and improve the possible response nonlinearities of all channels, since any imperfection will result in an increase of the constant term in the jet energy resolution [1];
- keep track of timing stability and provide the corrections in case of exceeding predefined level;
- ensure the transfer of energy calibration results from the test beam setup to the real data taking environment.

The principle of the electronic calibration system for the hadronic end-cap calorimeter in ATLAS closely follows the one used by end-cap EM calorimeter. The calibration pulser developed in Košice was tested during test-beams with prototype modules and module-0 of HEC during 1997-1998. It was proved that pulser fulfill all requirements, but because of unification of front-end electronics for all liquid argon calorimeters in ATLAS, the decision of implementing the unified calibration board [4] was taken. Therefore in all test-beams in the 1999-2000 years this board was used and all results presented here are from this tests.

2 CALIBRATION

The detailed studies of the influence of the calibration accuracy on the jet energy resolution - one of the main tasks of the HEC calorimeter - were made [1] as well. It turned out that imperfections of the electronics are propagated only to the constant term of the jet energy resolution formula. Therefore, to reduce an influence of the calibration system to a tolerable level, its accuracy must be better than 1 %. This requirement is approximately four times less stringent

than that for the EM calorimeter. On the other hand the requirements for measuring muons force the calibration system to be able to work in the extremely low signal region also.

2.1 General Layout

Longitudinally the readout cells of the HEC calorimeter are combined into four sections in ratios 8:16:8:8 (Fig. 1). A HEC calorimeter readout cell consists of two detector pads (EST structures ??). Each signal from an energy deposit in a readout cell is amplified by the preamplifier connected to it. 8 preamplifiers are combined into one MPI GaAs HEC chip. The signals of 4 or 8 preamplifiers resp. in one longitudinal section are summed up by a "summing amplifier", forming the signal of the readout channel.

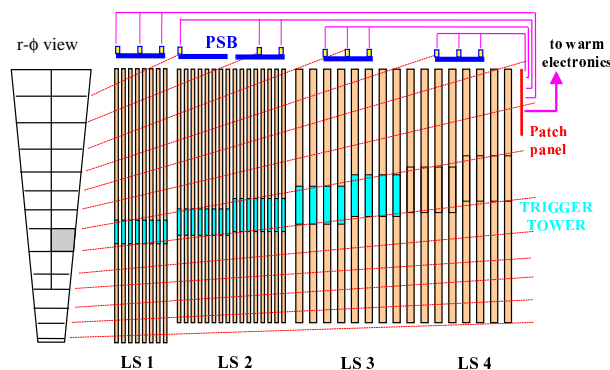


Figure 1: Layout of ATLAS HEC module

The voltage pulse of one generator is sent through high-quality 50 Ohms coaxial cable to the strip line board located close to the detector pads. To reduce the number of cables, one generator signal is splitted to three on the calibration distribution board (CDB) at the back plane of each module. Then each of these three signals pulses up to 32 readout cells (16 preamplifiers) through the corresponding calibration resistors simultaneously. Such a calibration scheme is sensitive to the attenuation of the signal in the cables. The strip line board is mounted parallel to the beam direction into the notch between two neighboring longitudinal sections in pseudo rapidity.

In addition this solution requires very good uniformity of the calibration signal distribution to the individual calibration resistors. Special studies were devoted to this topic,

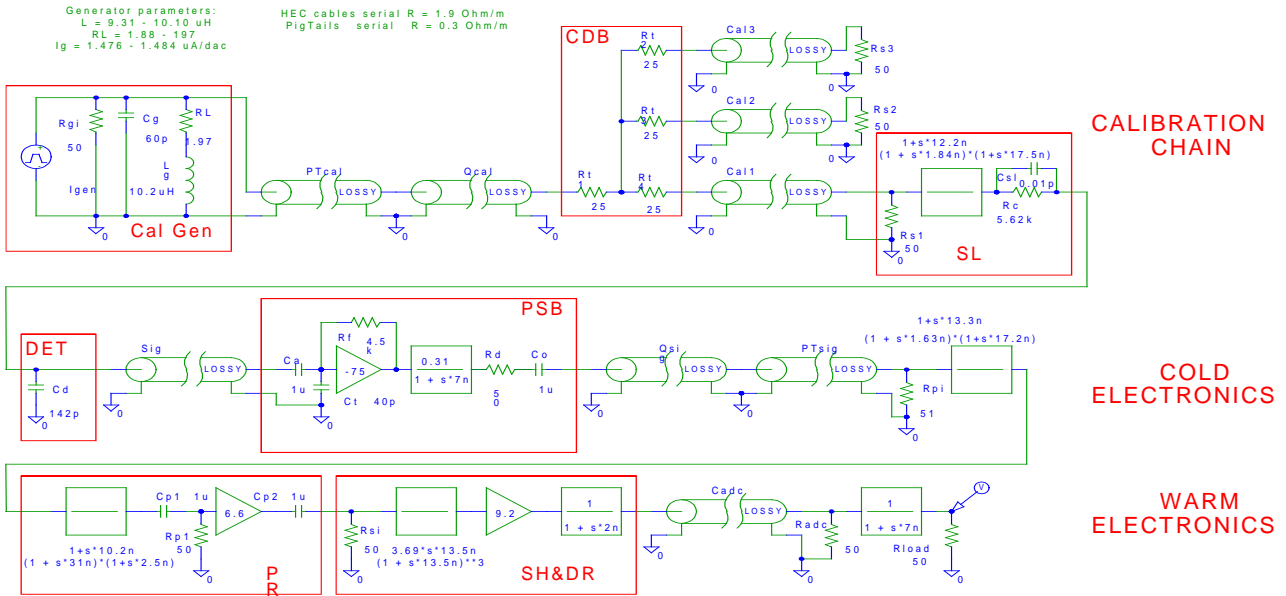


Figure 2: Electronic chain used in ATLAS HEC test-beams

which resulted into a design of a calibration strip line terminated by an adjusted termination resistor. The resulting inhomogeneity over the whole length of one strip line is less than 0.4 %.

2.2 Electronics chain

In order to meet all requirements and to understand the behavior of the full electronics chain, the special measurements, as well as simulations was performed. The basic elements of the chain (Fig. 2) are calibration pulser, splitting CDB, strip-line with calibration resistors, preamplifiers, preshapers, shapers, ADC's and of course various cables. All cables are final ATLAS length and type, so the chain used is very close to the final which will be used in ATLAS.

The parameters found for various part of chain are used in the parameterization of response function (see section Reconstruction). The signals form and dynamic range is sketched on Fig. 3

3 STEERING AND DATA TAKING

The setup for steering and data taking used during tests in H6 beam in North Area consist from two computers, VME steering and DAQ modules and calibration board (Fig. 4).

The computers are VME based RAID 8235 computer and EP-LX v.1.3 operating system, used as VME master for steering all VME based modules and the VME based HP 9000/743 computer, used for data storing and monitoring tasks. The Orsay version of the Calibration Board has big format for FE crate, holds 128 generators and communication is done via VME based SPAC module. Service Module (SM) is VME based clock server and synchronization module. It takes the external trigger requests (either

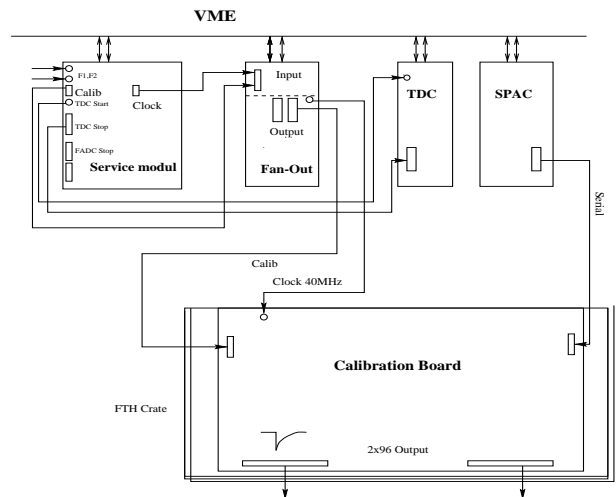


Figure 4: Calibration setup in ATLAS HEC test-beams

particle or calibration) and optionally synchronizes them with the clock. The output signals are

- the Start and Stop signals leading to the TDC module for trigger timing measurement
- the calibration and FADC clock signals
- the FADC stop signal.

The phase between the trigger and clock signal, used only during calibration running in asynchronous mode, is measured by TDC module.

The software developed for test beam usage evolved from old TGT[7] calibration steering to the present version running under EP-LX real time Unix clone and HP-UX operating systems. On Fig. 5 is sketched the software skeleton. The description of various modules follows.

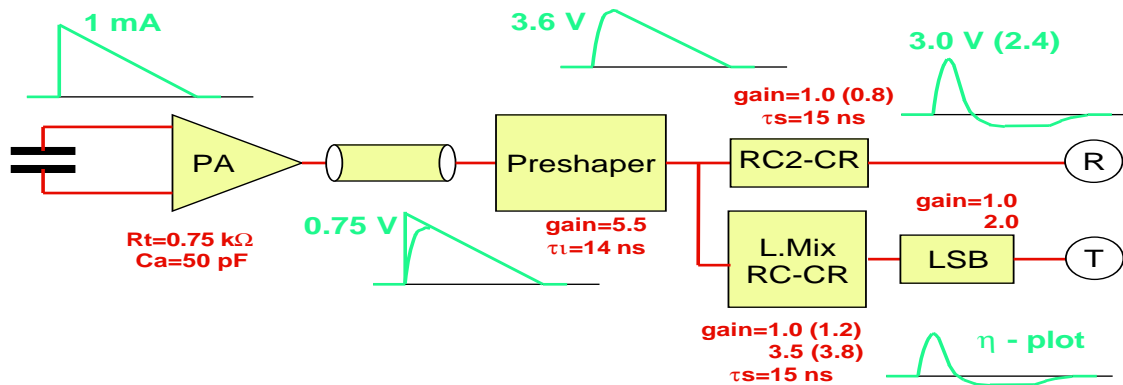


Figure 3: Signals and dynamic range

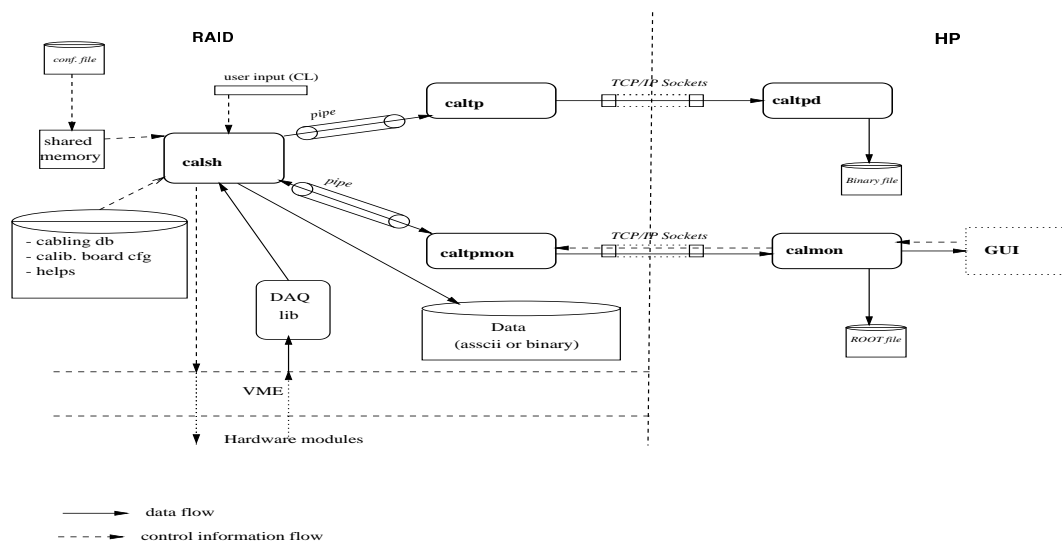


Figure 5: Software modules and connections

The basic software module is the calibration steering shell, called *calsh*. The main *calsh* tasks are:

- the interactive access to the hardware modules via command line interface
- to store the measured calibration data either in local file or send them out via TCP/IP connection
- the interpretation of the commands received from monitoring tasks i.e. performing required measurements and sending the results back

Calsh cooperates with the readout part of DAQ library and with the *caltp* and *caltpmon* modules, based on CALTCP Network Programmer's Library [9].

The purpose of *caltp* module is to transform the measured data into network format and, using the TCP/IP connection, transfer them to any machine where the *caltpd* daemon is running. The *caltpd* daemon is simple task, receiving the data stream from the network, transforming it to local format and storing it as binary file.

Another possibility is to drive the calibration runs remotely via network, which is used currently by monitoring programs.

The *calmon* module is ROOT based [10] monitoring module, which controls the basic parameters of electronics (pedestal, noise and signal level, compares those with reference values, and allow interactively inspect various views on the system. The module is using graphical user interface and is based on Object-Oriented technologies. *Calmon* use the services of *caltpmon* module to communicate with *calsh* and to get back the measured data. *Calmon* version which use the X-windows GUI, so called *Xcalmon* is used for per day control of the system during the data-taking.

There exist also the extended batch version of monitoring program, which was used in 1998 for three-month monitoring of cold electronics to meet the requirements for PRR [8]. The batch version is without user interface, running autonomously, collecting the data, performing basic analysis (shape fitting, gain computation) and storing the results in database.

The concept of calibration steering is to be a shell-like environment, to allow practically any type of measurements, which are needed in the time of setting up and debugging the electronics. The most typical measurements are listed here.

- continuously pulsing with defined signal level, without read-out, for oscilloscope measurements
- noise measurement with switching off the calibration generators and reading the software generated "random triggers"
- signal time position finding by varying the delay of calibration pulse and read-out timing
- cable-check with pulsing in sequence one by one all the calibration generators, looking for the signal in all channels, and comparing with cabling database
- quick signal check pulsing all the channels with constant pulse level
- signal shape measurement by performing delay-scan with fine delaying of calibration pulse through 25 ns sampling time
- gain and nonlinearity measurement pulsing all the channels with different pulse levels
- cross-talk measurements by pulsing one or few generators and reading all the neighboring channels

4 RECONSTRUCTION

Because the optimal filtering (OF) method for amplitude reconstruction [5] is assumed to be used in ATLAS, a knowledge of particle signal waveform is required. In order to be able to use measured calibration waveform for obtaining particle signal waveform, we have chosen to parameterize the impulse response of the read-out system.

The first choice, used for 1998 data, was based on the response function, expressed as the sum of "elementary" poles [6].

$$h(t) = \sum_{n=2}^{N_f} d_n f_n(t)$$

$$f_n(t) = \frac{t^{n-1}}{(n-1)!} \frac{e^{-\frac{t}{\tau_0}}}{\tau_0^n} \theta(t) \quad (1)$$

That time our knowledge of the electronics chain was not precise enough, so the calibration response was fitted with free parameters d_n . With $N_f=8$ the sufficient accuracy has been achieved. The problem with this parametrization is that the free parameters have no physical meaning and it was very hard to keep the stability and reproducibility of the fit. During 1998 and 1999 the detailed study of the chain components has been done that gave the possibility to fix many constants involved in 1. Following to the schematics on Fig. ??, the full expression of the calibration signal in s-domain can be obtained:

$$h(s) = \frac{1}{s} \cdot \frac{\alpha + s\tau_c}{1 + s\tau_c} \cdot \frac{1 + s\tau_{zc}}{(1 + s\tau_{pc})(1 + s\tau_{0c})} \cdot \frac{1}{1 + s\tau_d} \cdot \frac{1 + s\tau_{zs}}{(1 + s\tau_{ps})(1 + s\tau_{0s})} \cdot \frac{1}{1 + s\tau_i} \cdot \frac{s\tau_s}{(1 + s\tau_s)^3} \cdot \frac{1}{1 + s\tau_{dr}} \cdot \frac{1}{1 + s\tau_{0a}} \quad (2)$$

which after symbolic Inverse Laplace Transform leads to unreasonably long expression in time domain. There are two possible simplifications: (i) to calculate coefficients d_n numerically from function 2 and (ii) to simplify expression 2 to some reasonable level and use complete analytical expression in time domain. For the analysis of data 1999 the second approach was used. The simplified version of function 2 is:

$$h(s) = \frac{1}{s} \cdot \frac{\alpha + s\tau_c}{1 + s\tau_c} \cdot \frac{(1 + s \cdot \tau_Z)}{(1 + s \cdot \tau_p)(1 + s \cdot \tau_0)} \cdot \frac{1}{(1 + s \cdot \tau_D)(1 + s \cdot \tau_I)} \cdot \frac{s \cdot \tau_s}{(1 + s \cdot \tau_s)^3} \quad (3)$$

with free parameters τ_I and τ_s fitted in time domain on calib. data. Results of fitting the calibration signals, with the residual are on Fig. 6. We restricted the fitting region to the interval where 5 samples for the OF are located.

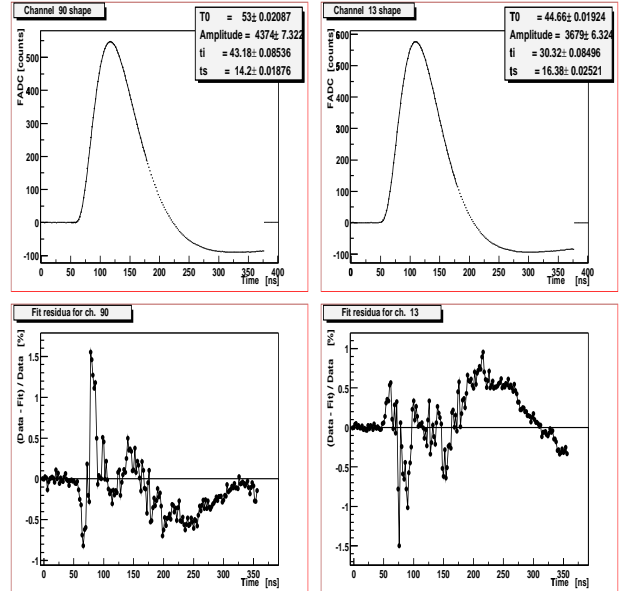


Figure 6: Results of calibration signal fit by function 4

The main problems still remain at the signal beginning and undershoot region, because of not taking into account the effects of X-talk and still not fully described effect of cables. Nevertheless the quality of shape fit is sufficient to produce the optimal filter coefficients both for calibration and particle signals shape. The calibration ramp fitted, together with fit residual, is on the Fig. 7

We see, that the largest residual, and still the main problem in the HEC calibration is the low signals region. Unfortunately, this is the region where the muon signal is expected, so it will be the main task in the near future to improve the description and correct analysis of low signals.

The first improvement, which is now work out, will be the developing of new procedure to obtain the particle signal shape "directly" from calibration shape, avoiding fitting, which will be presented on the CALOR2000 conference. The second improvement planned is the detailed

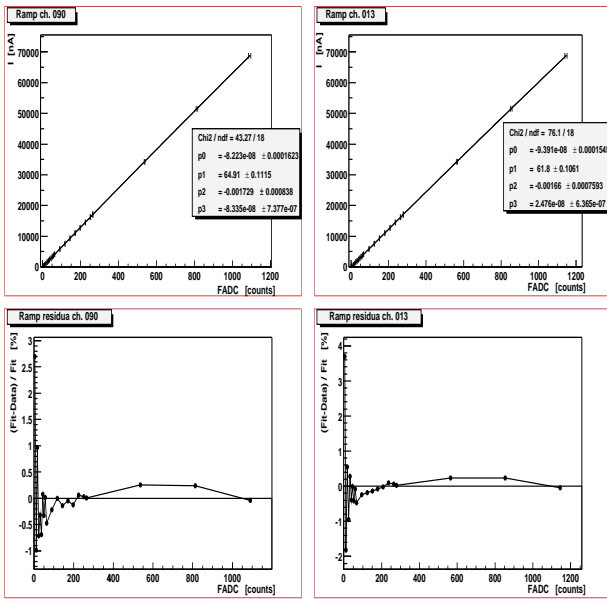


Figure 7: Example of calibration ramps fitting

study of low signals from calibration pulser and its appropriate description.

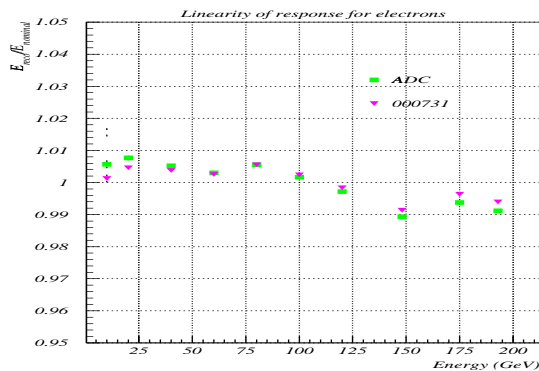


Figure 8: Linearity of the electron signals

But the present calibration procedure is working for the electrons well (see Fig. 8, triangles are calibrated amplitudes), and for pions sufficiently. The effect of X-talk to signal shape is shown on the Fig. 9, where shape when all generators are working simultaneously (there is the signal in all readout channels) is compared with the shape when only one generator is working (there is no signal in neighboring channels).

5 SUMMARY

The various tests of the full calibration chain for the ATLAS HEC was performed during last years both on site in the H6 cryostat and in lab. and description of all parts was found. Basically the system is well understood.

The procedure to obtain the particle signal shape from the calibration one, based on fitting the data by simplified version of response function (4) and to compute the optimal

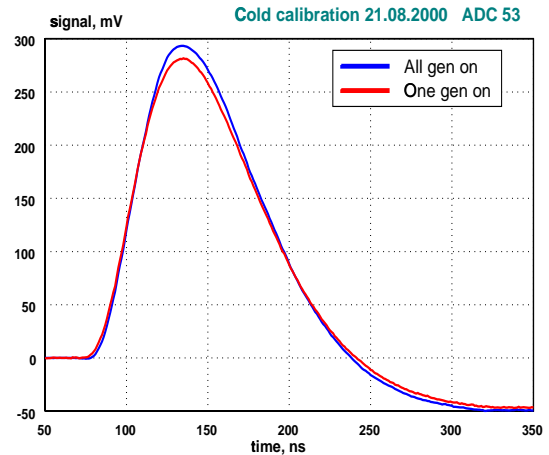


Figure 9: X-talk influence on the signal shape

filter coefficients, was set up. The results of test-beam data analysis shows, that procedure is working for electrons and pions well.

The improvement of this procedure is foreseen, mainly for the low signals reconstruction procedure, new method for computing the particle shape "directly" from calibration one implementation, and X-talk effects taking into account.

6 REFERENCES

- [1] A.E.Kiryunin, "The influence of characteristic parameters of the electronics chain of the ATLAS hadron end-cap calorimeter on the jet energy resolution", ATLAS Internal Note CAL-NO-064 (1994).
- [2] ATLAS Collaboration, "ATLAS Liquid Argon Calorimeter, Technical Design report", CERN/LHCC/96-41 (1996).
- [3] ATLAS Collaboration, "ATLAS Technical Proposal", CERN/LHCC/94-43 (1994).
- [4] G. Perrot, "The ATLAS Calorimeter Calibration Board", Proceedings LEB'99, CERN-99-09.
- [5] W.E. Cleland, E.G. Stern, "Signal processing consideration for liquid ionization calorimeters in a high rate environment", NIM **A338**(1994)467-497.
- [6] W.E. Cleland et. al., "Dynamic range compression in a liquid-argon calorimeter", 6th International Conference on Calorimetry in High-energy Physics : ICHEP '96 Frascati, Italy, Frascati physics series, 6(1996)849-860.
- [7] W. Braunschweig et al., RD33 Collaboration, "Performance of the TGT liquid argon calorimeter and trigger system", NIM **A378**(1996)479-494.
- [8] "Report on the HEC Cold Electronics Production Readiness Review", ATL-TC-ER-0013.
- [9] R. Chytráček: CALTCP 1.0 Unix Network Programmer's Library, <http://chytrace.home.cern.ch/chytrace/caltcp/>
- [10] Rene Brun and Fons Rademakers, ROOT - An Object Oriented Data Analysis Framework, Proceedings AIHENP'96 Workshop, Lausanne, Sep. 1996, NIM **A389**(1997)81-86. <http://root.cern.ch/>.